Binary and Ternary Particulate Composites. II. Tensile Behavior Over a Wide Range of Strain Rates

N. D. ALBEROLA,[1] Y. GERMAIN,[2] P. MELE[1]

[1] Laboratoire Matériaux Polymères et Composites, Université de Savoie, Bat Le Chablais, Campus de Savoie Technolac, 73376 Le Bourget du Lac, France

[2] ELF/ATOCHEM-CERDATO, 27470 Serquigny, France

Received 4 March 1996; accepted 26 June 1996

ABSTRACT: Tensile properties of both a binary material, i.e., polystyrene (PS) reinforced by 15 vol % of glass beads, and ternary composites, i.e., showing either a maleated styrene/ethylene-*co*-butylene/styrene copolymer or a styrene-*co*-methacrylic acid copolymer (SAMA) adduct at the PS/glass-beads interface, are analyzed at room temperature and over a wide range of strain rates. Because the poor quality of the adhesion at the PS/glass-beads interface, the fracture toughness of these binary composites is strongly reduced, whatever the strain rate. The presence of the rubbery interlayer does not change the deformation mechanisms of the composite and the work to break is not significantly enhanced. This results from the poor compatibility between PS and the rubbery interphase leading to the debonding of coated glass beads. The good adhesion quality at the interfaces between phases in the ternary composite showing the SAMA adduct, i.e., SAMA/glass-beads and PS/SAMA interfaces, hinders the decohesion phenomenon. This results in an improvement in both the transfer load and the maximum strength. © 1997 John Wiley & Sons, Inc. J Appl Polym Sci **63:** 1041–1046, 1997

INTRODUCTION

For some applications, it is of interest to reinforce polymers with particles to create particulate composites tougher than the polymer matrix. One method is to introduce rubbery inclusions into the polymer.[1–4] But at the same time, this also results in a significant decrease in the modulus. Then, to obtain composites tougher than the matrix and showing a stiffness of the same order of magnitude as the continuous phase, it was suggested to reinforce the polymer matrix by rigid fillers such as glass beads coated by a polymeric adduct, for example a rubbery interlayer.[4–6] Accordingly, mechanical behavior, i.e., modulus and ultimate properties, of such ternary particulate composites is governed by an interplay of properties of the polymer matrix, the inclusions, and the interphase, including the adhesion quality between phases.[4,7–9] In particular, the ability of the interphase to improve the transfer load could depend not only on the adhesion quality at the fillers/adduct interface but also on the compatibility between the interface and the polymer matrix.

In the first part of this paper, micromechanical properties of two kinds of ternary particulate composites, i.e., polystyrene (PS) reinforced by glass beads coated either by a rubbery adduct (a maleated styrene/ethylene-*co*-butylene/styrene copolymer, SEBS) or by a rigid coupling agent (a styrene-*co*-methacrylic acid copolymer, SAMA), were predicted by an original modeling to give evidence, subsequently, for interactions between phases. Thus it was concluded that because the SAMA interphase exhibits a better compatibility with the PS matrix than the SEBS adduct, it could improve the transfer load between phases.

In this work, the tensile mechanical behaviors

Correspondence to: N. D. Alberola

of these materials are investigated at room temperature and at various strain rates to verify the validity of the approach developed in part I of this paper.[10] In particular, the ultimate properties of the ternary composites will be analyzed and compared to those displayed by the binary material to show the influence of the adhesion quality at the interfaces between phases on both the nucleation and the growth of cracks within the matrix.

EXPERIMENTAL

Materials

PS homopolymer, provided by the ELF/ATOCHEM Company (CERDATO, Serquigny, France) is used as the matrix. Its characteristics are reported in Table I of part I.

Binary particulate composites are constituted of PS matrix reinforced by 15 vol % of glass beads sized by a silane coupling agent. Sized glass beads were provided by the Sovitec Company (Belgium).

Two kinds of ternary particulate composites are constituted by adding the two following adducts:

1. a rubbery interphase, i.e., SEBS, provided by Shell Company, and
2. a rigid interphase, i.e., SAMA, provided by ELF/ATOCHEM Company (GRL, Pau, France).

The characteristics of the polymers used in this study are reported in Tables I and II of part I of this paper.

Sample Preparation

Binary and ternary compounds were prepared by mixing the components in a twin-screw extruder (Haake-Rheocord 40) at 463 K.

Unfilled PS and compounds were molded at 473 K under high pressure as dog-bone-shaped specimens (10 mm wide, 2.5 mm thick, and 60 mm long in the gauge section).

Characteristics of binary and ternary composites are listed in Table II in part I of this paper.

Test Procedure

Low strain-rate tensile tests were performed at room temperature in a Schenck-Trebel RSA testing machine equipped with a strain gauge extensometer. Ten replicates were run for each kind of materials. The reported data are the average values. The load-elongation curves were converted into engineering stress–strain plots by dividing the measured load on the sample by the initial cross-sectional area of the specimen, and the elongation by the original gauge length. At low strain rates, tensile dilation measurements were performed on PS samples. Strain gauge extensometers were attached to the specimen to measure the changes in length and width that took place during the deformation. The strain in the third direction is assumed to be equal to the transverse strain.

Tensile experiments at high strain rates were performed at room temperature by means of a tensile VHS 56 servohydraulic machine provided by Schenck Company. The sample is gripped to a piston rod which can be displaced at a velocity in the 0.1–20 m/s displacement rate range. The position of the piston rod and then the displacement of the sample versus time can be assessed by both the usual transducer and an optical extensometer. The load is measured by means of a piezoelectric crystal ring of 25 kN in the fixture assembly. Then, for each strain rate, such a setup provides the evolution of both the load and the specimen displacement versus time. Such curves are converted into usual engineering stress–strain curves according to the method described above.

At both low and high strain rates, the three following parameters are determined: Young's modulus (E), calculated from the initial slope of the stress–strain curve, and the maximum stress (σ_{max}) and strain (ϵ_{max}) at break.

Microscopy observations of metallized samples were performed on a Philips 505 scanning electron microscope.

RESULTS AND DISCUSSION

Tensile Behavior of Unfilled PS

Figure 1(a) shows a typical tensile stress–strain curve recorded for unfilled PS at room temperature and at a low strain rate, for example 3.3 $10^{-3}s^{-1}$. On increasing the stress, unreinforced PS exhibits an elastic, then plastic, behavior characterized by a whitening of the sample occurring for strain levels higher than 1.5%. To identify the toughening mechanisms of PS in tensile mode, the volume changes occuring on deformation can be analyzed.[4,11] As a matter of fact, shear yielding

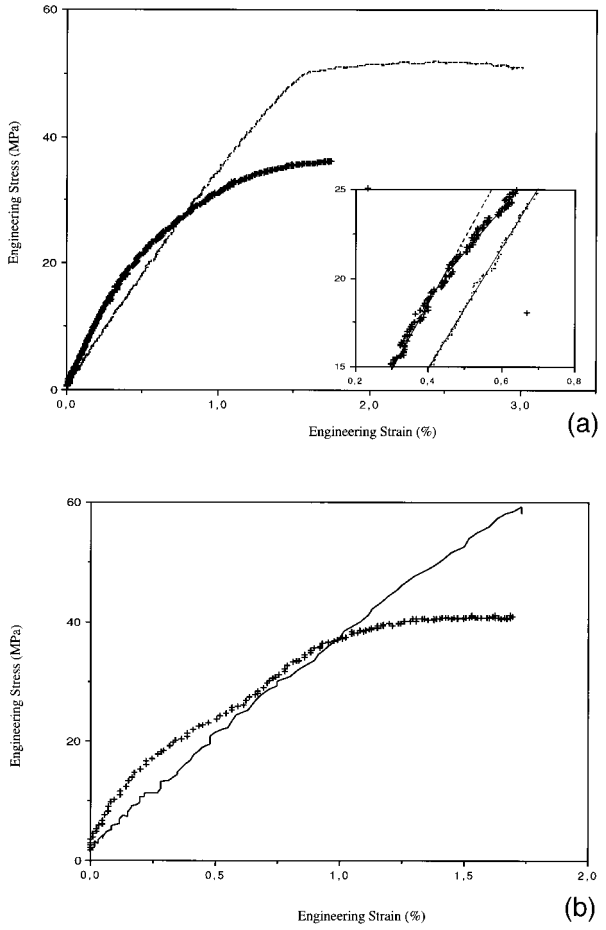

Figure 1 Stress–strain curves recorded at room temperature for unfilled PS (——) and binary PS/glass-beads composites (+) at the two following strain rates: (a) 3.3 $10^{-3}s^{-1}$; (b) 20 s^{-1}.

results in no dilation during the deformation, while both crazing and void formation do result in dilation. As shown in Figure 2, the rise in the volume strain occuring for strains greater than 1.5% versus the longitudinal strain has a slope of about 0.9, indicating that the plastic deformation is accompanied by dilation. It can then be concluded that at low strain rates, the plastic deformation of PS is mainly due to crazing but there is also a weak contribution of shear yielding.

The maximum strength of unfilled PS increases linearly with a constant slope versus the logarithm of the strain rate (Fig. 3). It can then be suggested that the craze nucleation in PS is governed by a single molecular mechanism over the analyzed strain-rate range. The ductile–brittle transition occuring for $\dot{\epsilon} = 20\ s^{-1}$ [Fig. 1(b)], could be related to changes in the mechanisms of craze breakdown. In fact, it is well known that

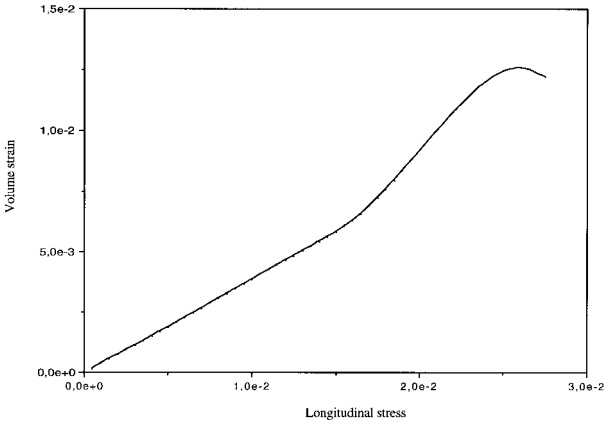

Figure 2 Volume strain versus longitudinal strain plot for unfilled PS at room temperature and at 3.3 $10^{-3}s^{-1}$.

fibrils, which bridge between the two bulk polymer–craze interfaces, can break down by the two following mechanisms: (1) the disentanglement of chains in the midrib, the layer of fibrils in the center of the craze, and (2) the chain scission at the bulk polymer–crazes interface.[12,13] Thus, in agreement with Plummer and Donald,[11] it can be suggested that at room temperature and at low strain rates, the fracture of the unfilled PS results mainly from the disentanglement of chains. With increasing the strain rate at room temperature, the craze fibril stability is reduced because of the kinetic character of the disentanglement phenomenon. In fact, at high strain rates, the motion ability of macromolecules is reduced; the chain scis-

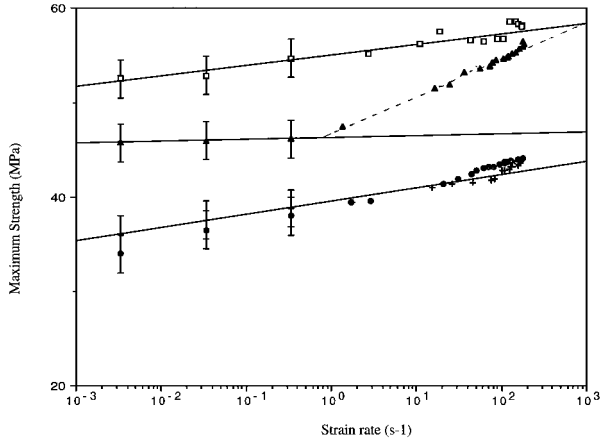

Figure 3 Maximum strength (σ_{max}) versus the logarithm of strain rate of unfilled PS (□), binary PS/glass-beads composites (+), ternary PS/SEBS/glass beads (●), and PS/SAMA/glass beads (▲).

sion mechanism is then favored over the disentanglement of the macromolecular chains.

Tensile Behavior of Binary Composites

Figure 1(a) shows the tensile behavior at room temperature and at a low strain rate, i.e., 3.3 $10^{-3}s^{-1}$, of the PS matrix reinforced by glass beads. The presence of glass beads induces an increase in Young's modulus but a decrease in both the maximum strength and the ultimate elongation. Moreover, an inflection can be detected in the stress–strain curve for about 12 MPa. In agreement with Vollenberg and Heikens,[14] such a decrease in the stiffness of the sample could be due to the debonding of glass beads from the PS matrix because of the poor adhesion quality at the fillers/polymer matrix interface. Moreover, because no significant change in the slope of the linear increase of σ_{max} with log $\dot{\epsilon}$ is detected for such a binary composite (Fig. 3), it can be concluded that nucleation of cracks in the composite is governed by the same molecular mechanism as that of controlling the deformation of the unfilled polymer. This result confirms that interactions between fillers and polymer matrix are weak. Such an interpretation is consistent with conclusions from the micromechanical analysis (see part I) and confirmed by the scanning electron micrograph of the fracture surface of PS/glass-beads composites [Fig. 4(a)], which gives evidence for the poor adhesion quality at the PS/glass-beads interface.

Accordingly, the decrease in the fracture toughness of the material induced by fillers could result from the poor interfacial adhesion at the polymer matrix/glass-beads interface which improves both the nucleation and the propagation of cracks. In fact, when particles are debonded from the matrix a small cap cavity is formed around the bead. This cavity could induce extra stress concentration. Craze nucleation can then occur for lower applied stresses. Moreover, in agreement with Kinloch and colleagues,[15] and Dekkers and associates,[8] it can be suggested that the weak interfacial adhesion between fillers and PS matrix could also impair the efficiency of the crack-pinning mechanism. In fact, when particles become debonded they are ineffectual as pinning positions, and crack propagation is favored.

Tensile Behavior of Ternary Particulate Composites

Figure 5 shows the tensile mechanical behavior at room temperature and at a low strain rate,

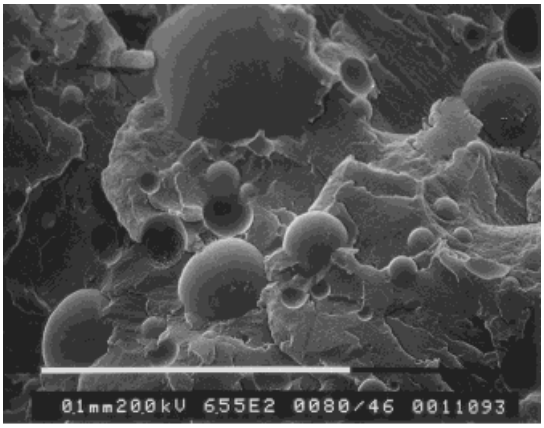

(a)

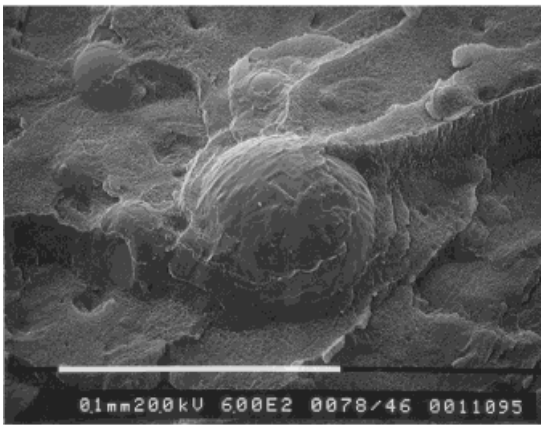

(b)

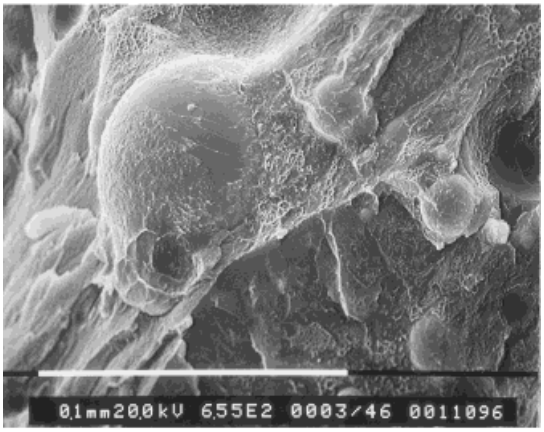

(c)

Figure 4 SEM micrographs of fracture surface of (a) PS reinforced by glass beads, (b) PS/SEBS/glass-beads composite, and (c) PS/SAMA/glass-beads composite.

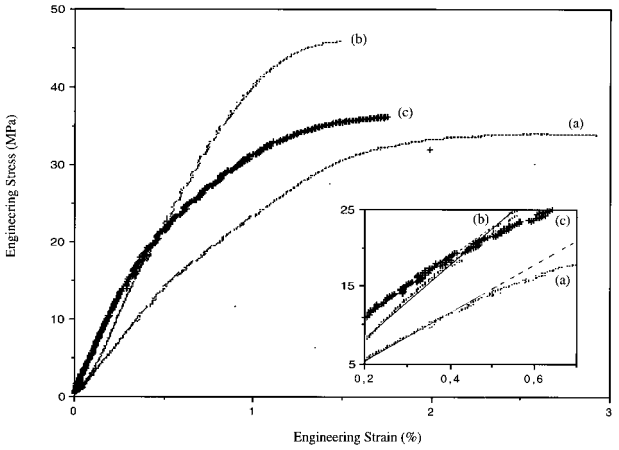

Figure 5 Stress–strain curves recorded at room temperature and at 3.3 $10^{-3}s^{-1}$ for ternary particulate composites showing (a) a maleated SEBS interphase, and (b) a SAMA interphase. Stress–strain curve recorded under the same conditions for binary PS/glass-beads composites (c).

i.e., 3.3 $10^{-3}s^{-1}$ of ternary composites showing the rubbery interphase. The stress–strain curve of the binary composite recorded in the same conditions is also shown for comparison.

The rubbery interfacial layer induces a decrease in Young's modulus and an increase in the fracture toughness of the material, characterized by a larger elongation at break and a maximum strength approximately equal to that of a binary composite. But it can be observed that the ultimate strain is not larger than that of unfilled PS. Then the work to break is not significantly increased by coating the beads with the rubbery adduct [Figs. 1(a) and (5)]. Moreover, for strains less than 2%, the stress–strain curve of such a ternary composite exhibits, as does the binary one, an inflection due to a decohesion phenomenon. The debonding stress is about 15 MPa. Because no significant change in the slope of the variation of σ_{max} versus log $\dot{\epsilon}$ is induced by the presence of the rubbery interphase, it can suggest that the presence of this rubbery interphase does not modify the the deformation mechanism of the matrix. This is consistent with weak interactions between the SEBS interphase and the PS matrix. The debonding phenomenon could then occur at the SEBS/PS interface. Such an interpretation agrees with conclusions from the micromechanical analysis. Scanning electron microscopy of the fracture surface of the PS/SEBS/sized glass beads gives evidence for a layer of resin on the particle surface, which could correspond to the rubbery adduct, showing good interfacial adhesion with glass beads [Fig. 4(b)].

Accordingly, it can suggested that the decrease in the maximum strength shown by this ternary composite with respect to that of displayed by the unfilled PS originates from the same cause as that invoked for the binary composite. In fact, the debonding of the coated glass beads improves the craze nucleation in the PS matrix. Moreover, compared with the binary material, the increase in the strain at break exhibited by the PS/SEBS/glass-beads composite could result from the rubbery character of the interphase which could hinder, in part, the crack growth within the matrix.

In contrast to the rubbery interphase, the SAMA interfacial adduct induces an increase in the maximum stress but a drop in the strain at break. Then, the fracture toughness is reduced compared with that displayed by both the unfilled PS and the binary composite showing the rubbery interphase. Furthermore, no discontinuity in the slope of the stress–strain curve can be detected for the composite showing the SAMA interphase. This can be due to the good quality adhesion between the SAMA interphase and not only the glass beads but also the PS matrix.

With increasing the strain rate, the maximum stress of this ternary composite increases linearly as a function of the logarithm of the strain rate (Fig. 3), but the rate sensitivity seems to be less than that displayed by unfilled PS or binary and PS/SEBS/glass-beads composites. It can then be suggested that the deformation mechanisms of the PS matrix could be slightly modified by the interactions between the SAMA interphase and PS matrix. Such an interpretation agrees with the conclusions from the micromechanical analysis (see part I). Micrographs of the surface fracture of the PS/SAMA/glass-beads composite are also consistent with such an interpretation [Fig. 4(c)]. In fact, a remaining resin layer can be observed on the glass-beads surface which could be constituted not only by the SAMA interphase but also by the PS matrix.

The increase in the maximum strength induced by the presence of the SAMA interlayer could then result from an improvement in the transfer load between glass beads and matrix because of the good adhesion quality between phases. The brittle character of the failure shown by the PS/SAMA/glass-beads composite, even at low strain rates, can result from a chain-scission mechanism which improves the crack propagation. In fact, because of the interactions between the SAMA interphase

and PS matrix, the motion ability of macromolecules can be reduced and then the chain-scission mechanism could be favored over the disentanglement of the macromolecular chains.

CONCLUSIONS

Through dilation measurements during tensile testing, it was shown that toughening mechanisms of unfilled PS are governed mainly by nucleation and propagation of crazes. The ductile–brittle transition observed for PS matrix at a strain rate of about 20 s^{-1} could be related to a change in the breakdown mechanism of fibrils. Thus, at lower strain rates, breakdown of fibrils could result from the disentanglement of chains in the midrib; whereas at strain rates higher than 20 s^{-1} it could be due to chain scission at the bulk polymer–crazes interfaces.

The reinforcement of PS by glass beads induces a decrease in both the maximum strength and the strain at break, and then a drop in the fracture toughness of the material. No significant change in the rate sensitivity of the PS is induced by the presence of glass beads. Then, the deformation mechanisms of the PS matrix are not modified; this could result from the weak interactions at the PS/glass-beads interface. This is well illustrated by the debonding of the particles from the PS matrix occuring at a strength of about 12 MPa, and is consistent with micromechanical analysis reported in part I. The decrease in the work at break observed for the PS/glass-beads composites could then result mainly from the poor adhesion quality at the fillers/polymer-matrix interface.

The rate sensitivity of the PS/SEBS/glass-beads composite is very close to that displayed by both the unfilled PS and the binary composite. Then, it was concluded that the mechanism governing the nucleation of crazes in the PS matrix is not changed by the presence of the rubbery interlayer because of the weak interactions between the SEBS copolymer and the PS matrix. The debonding phenomenon of coated glass beads from the PS matrix detected at a stress of about 15 MPa is consistent with both such a conclusion and the micromechanical analysis (see part I).

The presence of a SAMA interphase induces a significant increase in the maximum stress but strongly reduces the strain at break, even at low strain rates. Moreover, no decohesion phenomenon occurs in such ternary composites. This behavior is related to the good compatibility between the SAMA copolymer and the PS matrix leading to an improvement in the transfer load between phases. The brittle character of the failure displayed by this ternary composite could also originate from the interactions between the SAMA interphase and PS, which could reduce the motion ability of the macromolecular chains of the matrix. Thus the breakdown of craze fibrils could be governed mainly by the chain-scission mechanism, even at low strain rates.

REFERENCES

1. S. H. Spiegleberg, A. S. Argon, and R. E. Cohen, *J. Appl. Polym. Sci.,* **48,** 85 (1993).
2. J. S. Wu, S. Shen, and F. Chang, *Polym. J.,* **26,** 33 (1994).
3. C. B. Bucknall, A. Karpodinis, and X. C. Zhang, *J. Mater. Sci.,* **29,** 3337 (1994).
4. C. B. Bucknall, in *Toughened Plastics,* Applied Science Publishers, London, 1977.
5. M. E. J. Dekkers, J. P. M. Dortmans, and D. Heinkens, *Polym. Comp.,* **26,** 145 (1985).
6. N. Amdouni, H. Sautereau, J. F. Gerard, F. Fernagut, G. Coulon, and J. M. Lefebvre, *J. Mater. Sci.,* **25,** 1435 (1990).
7. A. C. Moloney, H. Kausch, T. Kaiser, and H. R. Beer, *J. Mater. Sci.,* **22,** 2, 381 (1985).
8. M. E. J. Dekkers, J. P. M. Dortmans, and D. Heikens, *J. Appl. Polym. Sci.,* **28,** 3809 (1983).
9. D. M. Bigg, *Polym. Comp.,* **8,** 2, 115 (1987).
10. N. D. Alberola, F. Fernagut, and P. Mele, *J. Appl. Polym. Sci.,* **63,** 1029 (1997).
11. M. A. Maxwell and A. F. Yee, *Polym. Eng. Sci.,* **21,** 4 (1981).
12. C. J. G. Plummer and A. M. Donald, *Macromolecules,* **23,** 3929 (1990).
13. A. C. M. Yang, C. K. Lee, and S. L. Ferline, *J. Polym. Sci.,* **30,** 1123 (1992).
14. P. H. T. Vollenberg and D. Heikins, in *Composites Materials,* H. Ishida and J. L. Koenig, Eds., Elsevier Sci. Pub., 1986.
15. A. J. Kinloch, D. Maxwell, and R. J. Young, *J. Mater. Sci. Lett.,* **4,** 1276 (1985).